Exceptional Oxygen Sensing Capabilities and Triplet State Properties of Ir(ppy-NPh_2)$_3$

Chris S. K. Mak,[†] Dominik Pentlehner,[‡] Mathias Stich,[§] Otto S. Wolfbeis,[§] Wai Kin Chan,*[,†] and Hartmut Yersin*[,‡]

Department of Chemistry, The University of Hong Kong, Pokfulam Road, Hong Kong SAR, People's Republic of China, and Institut für Physikalische und Theoretische Chemie and Institut für Analytische Chemie, Chemo- und Biosensorik, Universität Regensburg, 93040 Regensburg, Germany

Received February 9, 2009
Revised Manuscript Received April 6, 2009

Cyclometalated Ir(III) complexes are excellent triplet emitters used in efficient OLEDs[1−3] and sensing devices.[4−6] These materials are also the subject of several spectroscopic[7−10] and theoretical[11,12] investigations. The potential for applications of Ir(III) complexes in optical devices is determined by their electronic structures. The unique excited-state properties of Ir(III) complexes make these compounds particularly suitable for applications in oxygen sensing, e.g., for aerodynamic measurements and biomedical imaging. Therefore, it is important to study the electronic properties of these complexes in detail and to investigate the possibilities of tuning and optimizing the emission behavior, for example, by substitution of known compounds. In particular, the substitution of ppy ligands of Ir(ppy)$_3$ by ppy-NPh_2 has distinct effects on the photoluminescence behavior, such as energy shifts, changes in the emission decay time, and quantum yields. Moreover, the substitution leads to an effective shielding of the emitting core and−what is very important−makes the compound soluble in organic solvents. Synthesis and electroluminescence properties of Ir(ppy-NPh_2)$_3$ and related compounds have already been reported.[13−15]

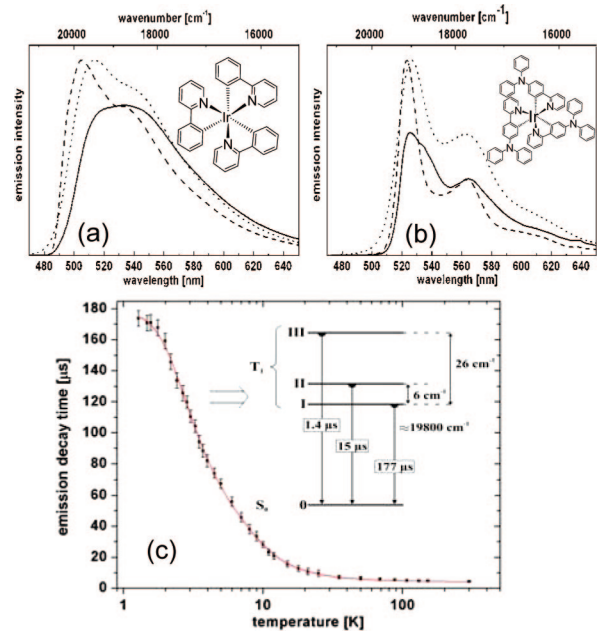

Figure 1. Emission spectra of (a) Ir(ppy)$_3$ and (b) Ir(ppy-NPh_2)$_3$ at 1.3 K (solid curve) and 10 K (dashed) in THF, and 300 K (dotted) in 2-MeTHF after UV excitation. The intensities of the different spectra are not comparable. The inset shows the molecular structures of Ir(ppy)$_3$ and Ir(ppy-NPh_2)$_3$. (c) Emission decay time of Ir(ppy-NPh_2)$_3$ in THF after pulsed excitation (λ_{exc} = 355 nm) versus temperature. The value at 300 K was measured for the complex doped into PMMA. The data given in the inset result from a fit of eq 1 to the experimentally determined data (points with error bars). The emission decay curves deviate slightly from monoexponential behavior due to distributions of the zero-field splittings and the individual decay times. The experimental data used represent the long decay components.

To obtain a better correlation and understanding of the nature of the excited states and of the photophysical properties, we investigate the triplet state properties of Ir(ppy-NPh_2)$_3$ also in comparison to those of Ir(ppy)$_3$ in detail and demonstrate the technological potential of Ir(ppy-NPh_2)$_3$ for oxygen sensing.

The emission spectra of Ir(ppy-NPh_2)$_3$ and Ir(ppy)$_3$ are compared and illustrated in Figure 1. The slightly more structured spectra and longer decay times found for Ir(ppy-NPh_2)$_3$ indicate a smaller MLCT (metal-to-ligand charge transfer) character of the emitting triplet state of the substituted complex compared to Ir(ppy)$_3$.[16−18] We note that the photoluminescence quantum efficiency ϕ_{PL} of Ir(ppy-NPh_2)$_3$ is very high and thus applications in OLEDs and sensors−as proposed below−are promising.

Detailed information about the emissive triplet state is obtained, if highly resolved spectra can be recorded. They would give direct insight into the electronic and vibronic structures of the involved electronic states.[18] However, well resolved spectra could not yet been obtained for Ir(ppy-

* Corresponding author. E-mail: waichan@hku.hk (W.K.C.); hartmut-yersin@chemie.uni-regensburg.de (H.Y.).
[†] The University of Hong Kong.
[‡] Institut für Physikalische und Theoretische Chemie, Universität Regensburg.
[§] Institut für Analytische Chemie, Chemo- und Biosensorik, Universität Regensburg.

(1) Yersin, H.; *Highly Efficient OLEDs with Phosphorescent Materials*; Yersin, H., Ed.; Wiley-VCH,: Weinheim, Germany, 2008.
(2) Baldo, M. A.; Lamansky, S.; Burrows, P. E.; Thompson, M. E.; Forrest, S. R. *Appl. Phys. Lett.* **1999**, *75*, 4.
(3) Adachi, C.; Baldo, M. A.; Forrest, S. R.; Thompson, M. E. *Appl. Phys. Lett.* **2000**, *77*, 904.
(4) Macro, G. D.; Lanza, M.; Pieruccini, M.; Campagna, S. *Adv. Mater.* **1996**, *8*, 576.
(5) Amao, Y.; Ishikawa, Y.; Okura, I. *Anal. Chim. Acta* **2001**, *445*, 177.
(6) Huynh, L.; Wang, Z.; Yang, J.; Stoeva, V.; Lough, A.; Manners, I.; Winnik, M. A. *Chem. Mater.* **2005**, *17*, 4765.
(7) Finkenzeller, W. J.; Yersin, H. *Chem. Phys. Lett.* **2003**, *377*, 299.
(8) King, K. A.; Spellane, P. J.; Watts, R. J. *J. Am. Chem. Soc.* **1985**, *107*, 1431.
(9) Colombo, M. G.; Brunold, T. C.; Riedener, T.; Güdel, H. U.; Förtsch, M.; Bürgi, H.-B. *Inorg. Chem.* **1994**, *33*, 545.
(10) Hofbeck, T.; Yersin, H. *3rd International Symposium on Molecular Materials−MOLMAT, Book of Abstracts*, Toulouse, France, July 8−11, 2008; p 157.
(11) Nozaki, K. *J. Chin. Chem. Soc.* **2006**, *53*, 101.
(12) Hay, P. J. *J. Phys. Chem. A* **2002**, *106*, 1634.
(13) Nishida, J.; Echizen, H.; Iwata, T.; Yamashita, Y. *Chem. Lett.* **2005**, *34*, 1378.
(14) Zhou, G.; Wang, Q.; Ho, C.-L.; Wong, W.-Y.; Ma, D.; Wang, L.; Lin, Z. *Chem. Asian J.* **2008**, *3*, 1830.
(15) Zhou, G.; Ho, C.-L.; Wong, W.-Y.; Wang, Q.; Ma, D.; Wang, L.; Lin, Z.; Marder, Todd B.; Beeby, A. *Adv. Funct. Mater.* **2008**, *18*, 499.
(16) Yersin, H. *Top. Curr. Chem.* **2004**, *241*, 1.
(17) Kalyanasundaram, K. *Photochemistry of Polypyridine and Porphyrin Complexes*; Academic Press: London, 1992.
(18) Yersin, H.; Finkenzeller, W. J. In *Highly Efficient OLEDs with Phosphorescent Materials*; Yersin, H., Ed.; Wiley-VCH,: Weinheim, Germany, 2008; Chapter 1.

10.1021/cm9003678 CCC: $40.75
Published on Web 05/04/2009

$NPh_2)_3$ even when the sample was cooled to $T = 1.3$ K and methods of luminescence line narrowing were applied. Panels a and b in Figure 1 show ambient and low temperature emission spectra of $Ir(ppy)_3$ and $Ir(ppy\text{-}NPh_2)_3$. The distinct changes of the emission spectra with temperature increase from $T = 1.3$ to 10 K are typically related to the population of a proximate higher lying state which exhibits dissimilar vibronic coupling properties with respect to the transition to the electronic ground state.[7,18] Interestingly, although the spectra are very broad, it is still possible to obtain information about the splitting of the triplet state into the three substates (I, II, III) and their individual emission decay times (τ_I, τ_{II}, τ_{III}) when the temperature dependence of the emission decay time is studied. This method has been successfully applied to $Ir(ppy)_3$[7,18] and several other organo-transition metal compounds.[19,20] For a thermally equilibrated system of three excited states, the experimentally easily accessible emission decay time τ_{therm} can be expressed by:[18−21]

$$\tau_{therm} = \frac{1 + e^{-\Delta E_{II/I}/k_B T} + e^{-\Delta E_{III/I}/k_B T}}{k_I + k_{II} e^{-\Delta E_{II/I}/k_B T} + k_{III} e^{-\Delta E_{III/I}/k_B T}} \qquad (1)$$

wherein $k_i = 1/\tau_i$ (with i = I, II, III) represents the individual decay rates for the transitions from the triplet substates to the electronic ground state 0, $\Delta E_{II/I}$ and $\Delta E_{III/I}$ are the energy separations between the substates (zero-field splittings, ZFS), k_B is the Boltzmann constant, and T is the absolute temperature.[18−21] Figure 1c shows the experimental data for $Ir(ppy\text{-}NPh_2)_3$ and the fitting curve according to the above equation. The fitting parameters are summarized in the energy level diagram shown in the inset. It is remarked that the value of $\tau_I = 177$ μs, representing the measured decay time at $T = 1.3$ K, has been kept fixed for the fitting procedure. We note that the emission properties at room temperature are determined by all three sublevels, though the properties are dominated by substate III because of its short decay time of 1.4 μs. Using the fitting parameters as determined for T ≤ 150 K and eq 1, a value of $\tau_{therm} = 4.1$ μs is obtained for $T = 300$ K. This value fits well to the $\tau = 4.3$ μs measured at ambient temperature for $Ir(ppy\text{-}NPh_2)_3$ doped into PMMA. The zero-field splitting of the T_1 state is caused by spin−orbit coupling (SOC), which induces quantum mechanical mixings of the three substates with higher lying triplets and singlets. In particular, the larger the singlet admixtures to a substate, the greater is its radiative emission decay rate and mostly its photoluminescence quantum efficiency. These effects are dominated by mixings to higher-lying ^{1,3}MLCT states.[18,20] The amount of ZFS is a measure of the MLCT character of the triplet state. This means, a triplet term (state) of an organo-transition metal compound with a large ZFS value, for example, more than ∼50 cm^{-1}, can be assigned to be dominantly of MLCT character, whereas a triplet with a small ZFS of only a few cm^{-1} or less can be assigned to be mainly of LC character.[16,18,20,22]

The photoluminescence quantum yield ϕ_{PL} of $Ir(ppy\text{-}NPh_2)_3$ was measured, using quinin sulfate (with $\phi_{PL} = 51\%$ in 0.1 N H_2SO_4) as quantum yield standard (see the Supporting Information). A value of $\phi_{PL} = 70\%$ was obtained in an oxygen-free environment, which is almost as high as the ϕ_{PL} value found recently for $Ir(ppy)_3$, $\phi_{PL} \approx 90\%$.[10]

Interestingly, the emission of $Ir(ppy\text{-}NPh_2)_3$ is efficiently quenched by oxygen. This is demonstrated by a drastic change of the emission decay time at ambient temperature in dependence of oxygen partial pressure. For example, in air-saturated 2-MeTHF (2-methyl-tetrahydrofuran) the emission decay time is as short as $\tau \approx 25$ ns. With deaeration, the τ value increases drastically up to 4.3 μs, which corresponds to an increase by a factor of approximately 170. In contrast, the emission decay time of $Ir(ppy)_3$ increases with deaeration under the same experimental conditions only from 22−25 ns to 1.5 μs. Thus, we expect that the dynamic range of response for $Ir(ppy\text{-}NPh_2)_3$ is by a factor of nearly three larger than that of $Ir(ppy)_3$ in oxygen sensing experiments.

$Ir(ppy\text{-}NPh_2)_3$ represents a highly promising candidate for oxygen sensing applications due to several reasons: (i) the compound exhibits a good solubility in organic solvents and organic polymers (in contrast to $Ir(ppy)_3$), since the diphenylamine substituents on the ppy ligand provides flexibility to the complex and promotes its solubility; (ii) the wide range of the excited state lifetime as a function of oxygen partial pressure results in a large dynamic range of response;[6] (iii) the high phosphorescence quantum yield of $\phi_{PL} = 70\%$ helps to obtain a high sensitivity of sensing devices; (iv) the relatively large complex $Ir(ppy\text{-}NPh_2)_3$ with its shielding substitutions is less sensitive to self-quenching or triplet−triplet annihilation effects than the smaller $Ir(ppy)_3$ complex; (compare also to ref 25) (v) $Ir(ppy\text{-}NPh_2)_3$ can be excited at 405 nm and is therefore compatible with low-cost LEDs as excitation sources, in contrast to often applied dye laser source; (vi) the large difference between excitation and emission energy allows for easy separation of the emission from the excitation light; (vii) the luminescence decay time in the microsecond range enables facile time-resolved imaging.[24]

For oxygen sensor preparation, a solution of 5 wt % $Ir(ppy\text{-}NPh_2)_3$ and 5 wt % ethyl cellulose (EC) in THF was used. EC was chosen as matrix polymer, because of its high oxygen permeability coefficient of 1.1×10^{-12} cm^2 Pa s^{-1}.[26] This type of polymer has excellent processability in common organic solvents and possesses good mechanical strength, photo-, and thermal stability. It is regarded as standard host material with good long-term stability for oxygen sensing.[27] The solution was sprayed on a solid support (aluminum plate) covered with a titanium dioxide basecoat as a reflecting layer for maximizing the emission signal.

A schematic drawing of the sensor layer is depicted in Figure 2. The sensor has highly sensitive response to the changes in oxygen partial pressure [O_2] due to the quenching

(19) Pentlehner, D.; Grau, I.; Yersin, H. *Chem. Phys. Lett.* **2008**, *455*, 72.
(20) Rausch, A. F.; Homeier, H. H. H.; Djurovich, P. I.; Thompson, M. E.; Yersin, H. *Proc. SPIE* **2007**, 66550F.
(21) Azumi, T.; O'Donnell, C. M.; McGlynn, S. P. *J. Chem. Phys.* **1966**, *45*, 2735.
(22) Finkenzeller, W. J.; Hofbeck, T.; Thompson, M. E.; Yersin, H. *Inorg. Chem.* **2007**, *46*, 5076.
(23) Lu, X.; Han, B.-H.; Winnik, M. A. *J. Phys. Chem. B* **2003**, *107*, 13349.
(24) Stich, M. I. J.; Wolfbeis, O. S. In *Springer Series in Fluorescence*; Wolfbeis, O. S., Resch-Genger, U., Eds.; Springer: Berlin, 2008; Vol. 5.
(25) Burn, P. L.; Lo, S.-C.; Samuel, I. D. W. *Adv. Mater.* **2007**, *19*, 1675.
(26) Pauli, S. In *Polymer Handbook*; Bandrup, J., Immergut, E. H., Grulke, E. A. , Eds.; Wiley-VCH: New York, 1999.
(27) Amao, Y. *Microchim. Acta* **2003**, *143*, 1.

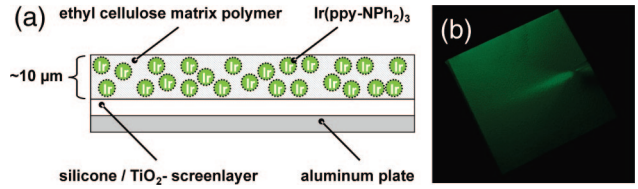

Figure 2. (a) Schematic diagram of the sensing layer. (b) $Ir(ppy\text{-}NPh_2)_3$ shows a high phosphorescence quantum yield of 70%. Its emission is strongly quenched by oxygen. This is illustrated on a photograph of a sensor using $Ir(ppy\text{-}NPh_2)_3$ under UV light with a nitrogen stream coming from the right.

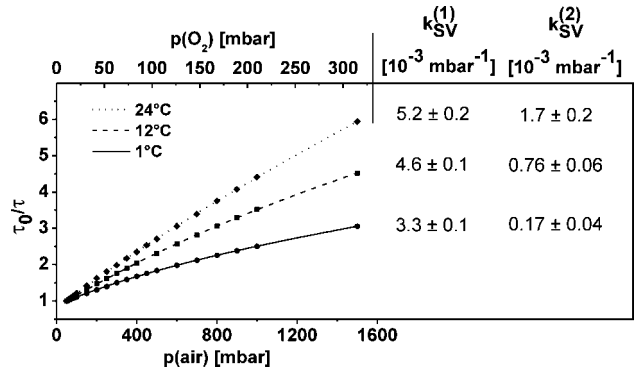

Figure 3. Stern−Volmer plots of quenching by oxygen at different temperatures. The obtained Stern−Volmer constants (with $f_1 = 0.85$ and $f_2 = 0.15$) are shown at the right-hand side. p(air) and $p(O_2)$ represent the pressure of air and the partial pressure of oxygen, respectively.

of luminescence by oxygen. (Figure 3) The changes in emission decay time were investigated for the range between 50 mbar and 1500 mbar of air pressure, corresponding to a range of oxygen partial pressures from 10 mbar to 315 mbar. For these measurements, the sensor was mounted in a thermostatted calibration chamber. The probe was excited with a 405 nm LED (pulse duration 20 μs) and the luminescence was detected by a cooled CCD camera. Luminescence decay times were determined by applying the "rapid lifetime determination" method using intensity images recorded for two different time delays (same gate time 2 μs) and assuming a monoexponential decay behavior.[28,29]

In Figure 3, Stern−Volmer plots displaying the dependence of the emission decay time on air pressure (and oxygen partial pressure) are shown for different temperatures. A strong dependence on air pressure is apparent. The efficiency of the sensor response can be described by Stern−Volmer plots when a bimolecular quenching mechanism is assumed. In this respect, it is remarked that the dopant (emitter) can have a large number of different microenvironments inside the polymer matrix. However, it turns out empirically that it is often adequate to take only two specific environments into account. Thus, a two site model is obtained, leading to[30,31]

$$\frac{\tau}{\tau_0} = \frac{I}{I_0} = \frac{f_1}{1 + k_{SV}^{(1)}[O_2]} + \frac{f_2}{1 + k_{SV}^{(2)}[O_2]} \qquad (2)$$

wherein f_1 and f_2 are the emissive fractions of the probe molecules in the different environments, $k_{SV}^{(1)}$ and $k_{SV}^{(2)}$ are the Stern−Volmer quenching constants in these environments and $[O_2]$ is the oxygen partial pressure. τ and τ_0 represent the measured decay time at a pressure $[O_2]$ and at zero $[O_2]$ pressure, respectively. In the first step of the fitting procedure, using the data set for a fixed temperature (e.g., at 1 °C), the emissive fractions were determined as $f_1 = 0.85$ and $f_2 = 0.15$ (with $f_1 + f_2 = 1$). Subsequently, the Stern−Volmer constants were determined for different temperatures using the same values for f_1 and f_2. (Figure 3) Both quenching constants, $k_{SV}^{(1)}$ and $k_{SV}^{(2)}$, increase with temperature. In principal, this behavior can be due to two effects, namely an increase in the radiationless deactivation of excited states of the emitter[32] and/or the increase in the oxygen diffusion rate through the polymer. For $Ir(ppy\text{-}NPh_2)_3$, however, the emission decay time in the absence of oxygen is almost independent of the sample temperature in the temperature interval from 1 to 24 °C. Therefore, it is concluded that the Stern−Volmer quenching rate constants are controlled by the diffusion of oxygen through the polymer.[33] We note that the quenching is diffusion controlled even up to relatively high air pressure of at least 1500 mbar, which represents an important property for a number of sensor applications.

In conclusion, we present triplet excited-state properties and oxygen sensing capabilities of $Ir(ppy\text{-}NPh_2)_3$. The observed changes of the photophysical properties of the derivative of $Ir(ppy)_3$ are ascribed to the electron donating properties of the diphenylamino substitutions. This causes a red shift of the emission, leads to a smaller MLCT character of the emitting state, and results in a longer emission decay time. In particular, $Ir(ppy\text{-}NPh_2)_3$ exhibits favorable sensing properties for oxygen because of its reasonably long emission lifetime, high luminescence quantum yield, and its good solubility in organic solvents and in organic polymers. Dissolved in ethyl cellulose, $Ir(ppy\text{-}NPh_2)_3$ displays high sensitivity on changes of oxygen partial pressure even for high air pressures of at least up to 1500 mbar. The sensor material may be used in fiber optic sensors,[34] microplates,[35] and−if cast on surfaces of aircraft models, for example−for imaging of air pressure distributions on surfaces.[28]

Acknowledgment. This work was supported by the BMBF and by a grant from the Germany/Hong Kong Joint Research Scheme Sponsored by the Research Grant Council (RGC) of Hong Kong and the German Academic Exchange Service (DAAD) (Ref. G_HK021/06). Financial support from the RGC (Project HKU 7008/07P) and the Strategic Research Theme (U of HK) is also acknowledged.

Supporting Information Available: Experimental details of the synthesis, descriptions of photophysical measurements and data for $Ir(ppy)_3$, $Ir(ppy\text{-}NPh_2)_3$ and the heteroleptic compounds $Ir(ppy)_2(ppy\text{-}NPh_2)$ and $Ir(ppy)(ppy\text{-}NPh_2)_2$, as well as a description of the preparation of the oxygen sensor (PDF). This material is available free of charge via the Internet at http://pubs.acs.org.

CM9003678

(28) Ballew, R. M.; Demas, J. N. *Anal. Chem.* **1989**, *61*, 30.
(29) Moore, C.; Chan, S. P.; Demas, J. N.; DeGraff, B. A. *Appl. Spectrosc.* **2004**, *58*, 603.
(30) Carraway, E. R.; Demas, J. N.; DeGraff, B. A.; Bacon, J. R. *Anal. Chem.* **1991**, *63*, 337.
(31) Draxler, S.; Lippitsch, M. E. *Anal. Chem.* **1996**, *68*, 753.
(32) Demas, J. N.; DeGraff, B. A. *Anal. Chem.* **1991**, *63*, 829A.
(33) Klessinger, M., Michl, J. *Excited States and Photochemistry of Organic Molecules*; Wiley-VCH: Weinheim, Germany, 1995.
(34) Wolfbeis, O. S. *Anal. Chem.* **2004**, *76*, 3269.
(35) Arain, S.; John, G. T.; Krause, C.; Gerlach, J.; Wolfbeis, O. S.; Klimant, I. *Sens. Actuators, B* **2006**, *113*, 639.